Geomech. Geophys. Geo-energ. Geo-resour. (2023) 9:90
https://doi.org/10.1007/s40948-023-00629-w

RESEARCH

Evaluation of excavation method on point load strength of rocks with poor geological conditions in a deep metal mine

Pingkuang Luo · Xugang Fang · Diyuan Li · Yisong Yu · Huahua Li · Peng Cui · Jinyin Ma

Received: 15 November 2022 / Accepted: 17 June 2023

Abstract In the field of deep mining engineering, it poses a challenge to promptly determine the mechanical properties of rocks under poor geological conditions through in-situ tests. However, the indirect determination of uniaxial compressive strength (UCS) of rocks can be achieved through the point load strength index (PLSI) test on irregular samples. In the present study, laboratory uniaxial compressive and field PLSI tests were carried out on irregular ore and rock blocks extracted through mechanical mining methods from a stope at a lead–zinc mine in Yunnan Province, China, with a depth of approximately 1000 m. The effects of mechanical excavation and drilling-blasting methods on the PLSI of rocks and ores are compared. It is found that there are significant differences in the point load strength indexes obtained by different excavation methods, and the $I_s(50)$ obtained after the mechanical excavation method approximates the actual value of ore and surrounding rocks. Two correction methods were utilized to obtain the point load strength indexes $I_{s(50)\text{-}1}$ and $I_{s(50)\text{-}2}$ of irregular rock samples. The correlation factors (k) linking $I_{s(50)}$ to UCS and Brazilian splitting strength are derived based on testing results. The findings indicate that using the conversion factor (k) recommended by ISRM to predict the UCS of rocks may significantly underestimate the actual strength of rocks in intricate mining environments. This study can serve as a benchmark for analogous deep mining projects.

P. Luo · D. Li (✉) · Y. Yu · J. Ma
School of Resources and Safety Engineering, Central South University, Changsha 410083, China
e-mail: diyuan.li@csu.edu.cn

X. Fang · P. Cui
Yunnan Chihong Zinc & Germanium Co., Ltd., Huize 654200, Yunnan, China

Y. Yu · H. Li
CINF Engineering Co., Ltd., Changsha 410019, Hunan, China

Article Highlights

- The laboratory UCS and field PLSI tests were carried out for the ore and rock blocks from a stope with about 1000 m depth.
- The point load strength indexes Is(50) of irregular rock samples were obtained by two correction methods.
- The influence of the excavation methods of mine stope on the Is(50) of rocks were analyzed.
- The correlation between Is(50) and UCS of irregular rock samples were built for the deep mine.

Keywords Deep mine · Point load strength index · Irregular lump test · Excavation method · Poor geological conditions

Published online: 29 June 2023

1 Introduction

The fundamental mechanical parameters of rocks, such as uniaxial compressive strength (UCS), tensile strength, cohesion, and internal friction angle, play a crucial role in ensuring the safe excavation and stability analysis of surrounding rocks in deep mines and rock engineering (Feng et al. 2020; Li and Zhao 2021; Qiany and Lin 1987; Zhang et al. 2022). The precise and expeditious determination of these parameters directly improves production safety and reduces project costs. UCS has been regarded as the most important mechanical parameter of rocks (Aladejare et al. 2022; Basu et al. 2010), and the quick degermation of this parameter holds paramount significance in deep mining and tunnelling engineering (Yin et al. 2017). However, laboratory tests to obtain UCS are expensive, time-consuming, and require a large number of standard rock samples (Diamantis et al. 2009). In addition, geological conditions in deep engineering, such as joint development, highly fractured rock masses, core discing, etc. (Xiao et al. 2021; Zhou et al. 2022; Zou et al. 2022)., are harsh and complex, making it challenging to prepare standard rock samples from deep in-site engineering. Consequently, quick determination of the UCS of rocks through laboratory tests is difficult.

This method has gained widespread acceptance due to its convenience, efficiency, economy, and applicability in field settings.

Due to the aforementioned reasons, the method of measuring UCS of rocks has gradually been replaced by more straightforward, expeditious and cost-effective test methods, such as point load tests (Protodyakonov 1960). The method to obtain the point load strength index (PLSI) using the point load (PL) test on rock samples, which in turn enables the indirect determination of both tensile (BTS) and UCS. This method has gained widespread acceptance due to its convenience, efficiency, cost-effectiveness and applicability in field settings (Heidari et al. 2012; Liu et al. 2018; Singh et al. 2012). Numerous scholars have examined the correlation between PLSI and UCS values of rocks based on rock properties and found that the size of rock samples significantly affects PLSI (Brook 1980; Fener et al. 2005; Kahraman et al. 2009; Rabat et al. 2020a). Li and Wong (2013) carried out radial and axial point load tests on metamorphic siltstone and sandstone to obtain their PLSI, and the relationships between PLSI and UCS as well as BTS were established. Basu et al. (2006, 2008) conducted PLSI tests on schistose rocks to examine their applicability and reliability in predicting UCS. Khanlari et al. (2014) determined the strength of five types of anisotropic bedded rocks using different testing techniques, and preliminarily found the relationship between the point load strength of bedded rocks and BTS. Masoumi et al. (2018) studied the size effect on the mechanical properties of intact rocks using point load tests on six different rocks, and concluded that the strength of rocks decreased with increasing size.

The concept of utilizing the point load test to obtain strength characteristics of irregular rock lumps was originally introduced by Protodyakonov (1960) in Russia. Over the past few decades, this method has been extensively applied in the fields of tunnel engineering, civil engineering and mining engineering. Liu et al. (2018) selected irregular rock block samples generated by tunnelling boring machine (TBM) to determine the PLSI by point load tests, and to obtain the UCS by drilling the rock core at the corresponding position. The findings indicate that the hob inflicted harm that diminished the strength of the rock block to 63.25% of the intact core sample. Kahraman (2014) performed point load tests and uniaxial compression tests on soft irregular pyroclastic rocks, and found an evident exponential correlation between UCS and PLS of rocks in both saturated and dry states. Xie et al. (2021) conducted point load test and indentation test on irregular rock fragments generated during tunnel excavation. They investigated the effects of indenter diameter and fragment size on the PLSI, and analyzed the correlation between PLSI and UCS. The water content, weathering degree, acidity and alkalinity of the environment, and temperature of rocks are also influential factors that impact the strength of rocks (Robertson et al. 2021; Su et al. 2021), which has been extensively studied in recent years. For example, Rabat et al. (2020b) designed five distinct levels of environmental relative humidity to carry out an experimental study through an improved vapour equilibrium technique, and systematically evaluated the influence of environmental relative humidity on the UCS, elastic modulus and PLS of calcarenite. Kohno and Maeda (2012) conducted point load tests and uniaxial compression tests on 44 different types of hydrothermally altered soft rocks, and pointed out that there was a strong exponential

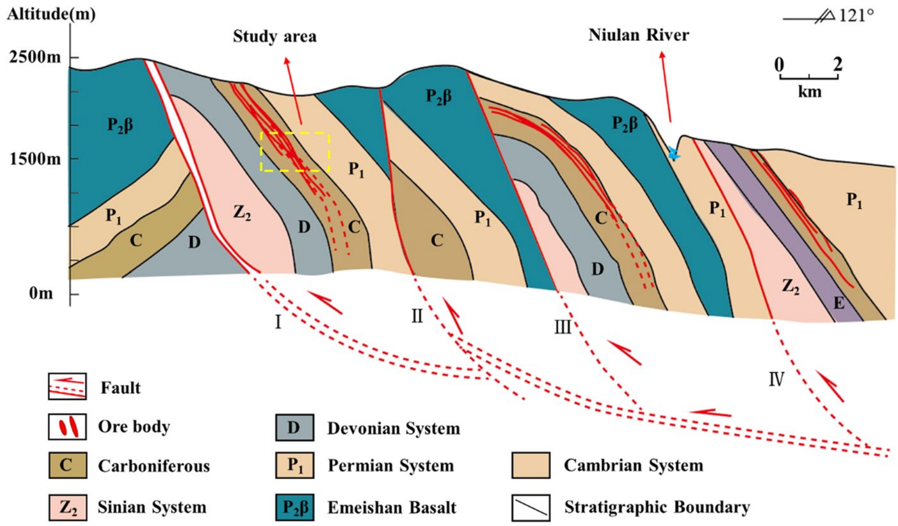

Fig. 1 Longitudinal profile of the geological structure and ore body distribution of the lead–zinc mine, modified and redrawn according to Han et al. (2014)

relationship between PLSI and USC for both dry and saturated rocks. Yin et al. (2017) experimentally investigated the effect of different weathering grades on the strength of granite. Sarici and Ozdemir (2018) further took the effect of freeze–thaw cycles into consideration, and the results demonstrate that as the number of freeze–thaw cycles increased, the porosity of the rock expanded, and its point load strength decreased.

Previous studies have primarily focused on the influences of external natural conditions, such as temperature and water, on the point load strength of rocks. However, limited research has been conducted on the effects of underground excavation disturbance, such as blasting vibration and mechanical excavation vibration, on the point load strength of rocks. Furthermore, most studies have only utilized a single correction method to optimize PLSI, ignoring the potential influence of correction methods on test results.

In this paper, point load tests were carried out on irregular rock and ore samples generated by different excavation methods at a deep mine in Yunnan Province, China. The effects of mechanical excavation method and drilling-blasting method on the PLSI of rocks and ores were compared. Various data analysis methods were used to compare the effect of correction coefficients on the distribution characteristics of PLSI. The findings of this study can serve as a valuable reference for similar deep mining projects and provide a solution to the challenge of obtaining rock mechanical properties in areas with poor geological conditions where standard rock and core samples are difficult to obtain.

2 Geological conditions and mining background

2.1 Geology

The metal mine is situated in Huize, Yunnan Province, China. Currently, its mining depth has reached -1500 m and is projected to reach – 2500 m in the future. With the increasing mining depth, the work environment of mine stopes becomes increasingly complex. The maximum horizontal principal stress of deep surrounding rocks has reached approximately 60.5 MPa, which brings huge challenges to safe and efficient mining production.

As shown in Fig. 1, the lead–zinc deposit of the study area is located at the northeastern end of the I tectonic zone, on the upper plate of the reverse fault, and on both flanks of the I backslope. The ore body is deeply buried and primarily situated in the Upper Paleozoic Carboniferous Baizuo Formation, with intricate geological conditions arising from the development of joints and fissures in the mine area. In addition, the total strike length of the ore body is approximately 1,700 m with an inclined extension of approximately 1,600 m, rendering it a substantial lead–zinc deposit. The ore body is of high-grade and has a high mining value, but the complex and poor geological environment such as high ground stress,

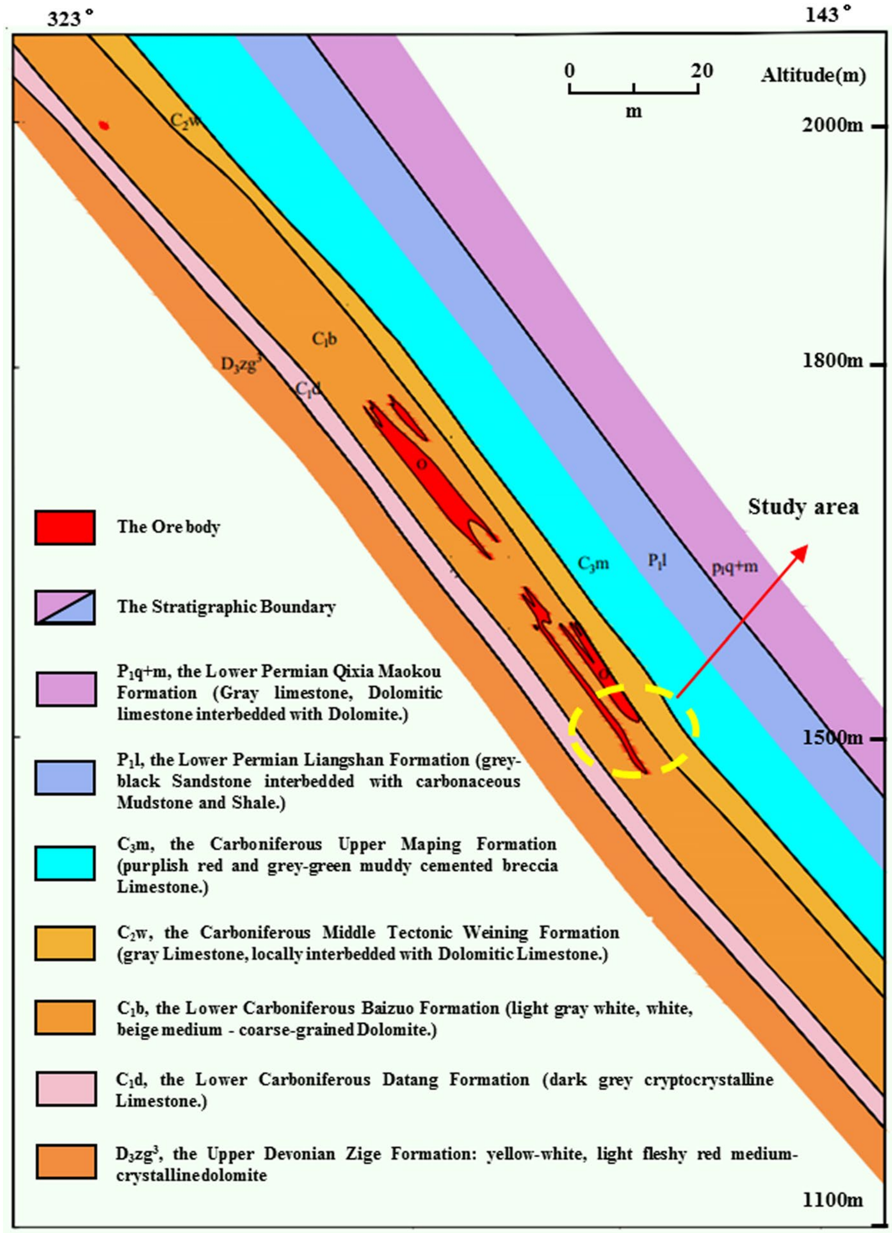

Fig. 2 The longitudinal profile of the study area (provided by CINF Engineering Co., Ltd.)

groundwater pressure and joint fracture development dramatically exacerbates the mining difficulties.

Figure 2 shows the longitudinal profile of the study area in this paper. The mining depth in this region is about 1000 m and is predominantly located within the Lower Carboniferous Baizuo Formation (C_1b). C_1b is in integrated contact with the Lower Datang Formation with a thickness of 50–60 m. The prevalent rock types in this area are gray chert and light gray-white and coarse-crystalline dolomite.

2.2 Mining background

As shown in Fig. 3, prevalent excavation methods in mining engineering comprise of drilling-blasting and mechanical excavation methods. To augment the productivity of the subterranean metal mine and guarantee the safety of laborers, the excavation method is being transitioned from the original drilling-blasting method to the mechanical excavation method. The mechanical excavation method offers the benefits of

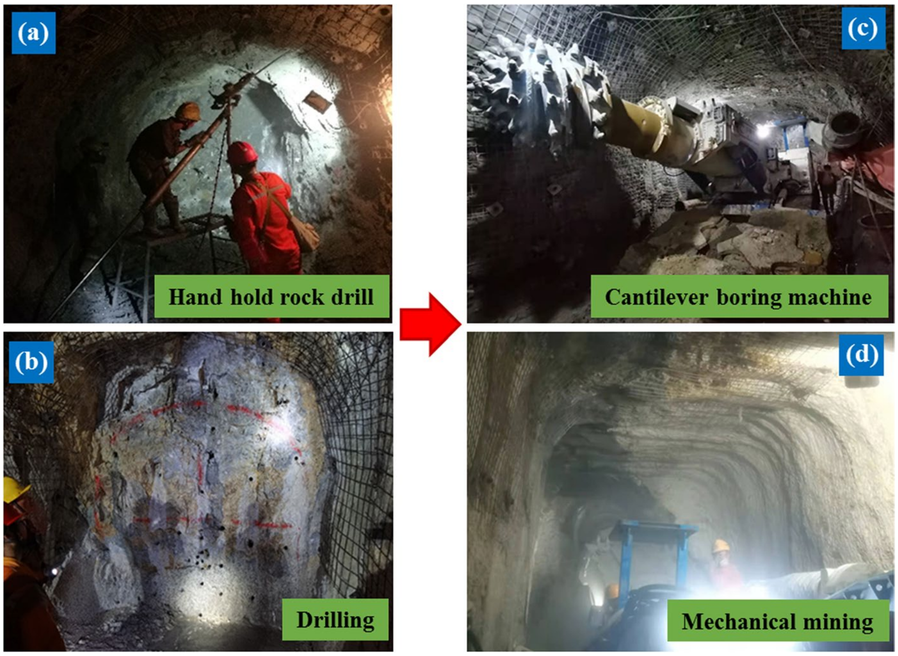

Fig. 3 Change from drilling and blasting method to mechanical excavation method: **a**, **b** drilling and blasting method; **c**, **d** mechanical excavation method

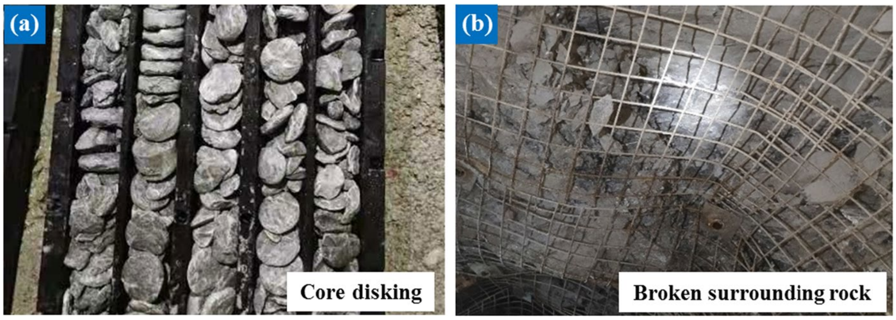

Fig. 4 Poor geological phenomenon in the deep lead–zinc mine: **a** core disking phenomenon when borehole drilling in a deep stope, and **b** rock falling at the roof in a deep stope

high efficiency, low expenses, and heightened safety. However, the high strength of rocks can result in severe wear and tear on mechanical equipment. Therefore, it is crucial to expeditiously and precisely obtain the strength of rocks for the mechanical excavation method.

To ascertain the mechanical properties of rocks, standard laboratory procedures typically involve conducting uniaxial compression tests and the Brazilian tensile tests. However, these laboratory tests necessitate the acquisition of standard rock samples (Han et al. 2022; Wong et al. 2017). Unfortunately, obtaining intact rock cores proves to be a challenging task when drilling boreholes in high-stress rock masses, particularly in deep mines with poor geological conditions (Han et al. 2023; Mohamad et al. 2022; Singh et al. 2012).

Illustrations of typical brittle failure in hard rocks at great depths in mines are presented in Fig. 4. With the increasing mining depth, hard rocks are more prone to spalling in the sidewall, and core disking commonly occurs during borehole-drilling under high in-situ stresses (Xiao et al. 2021). In addition, the developments of primary joints and fissures in deep surrounding rocks makes it arduous to obtain standard rock samples (Çobanoğlu et al. 2008). The point load test can be carried out using irregular rock samples in the field, which can avoid the unfavorable factors for sample preparation (Bieniawski 1975; Broch and Franklin 1972; Sarici and Ozdemir 2018). The

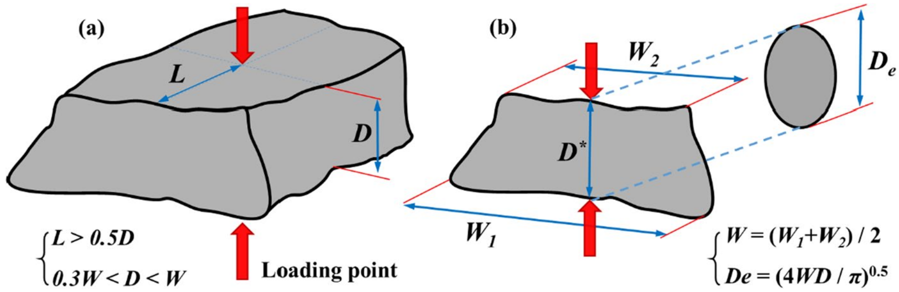

Fig. 5 Dimensions and equivalent diameter for irregular samples (Şahin et al 2020). **a** Diagram of an irregular sample; **b** Section through loading points

PLSI tests can determine the strength characteristics of deep rocks in a timely and accurate manner (Heidari et al. 2012).

3 Methodology

3.1 Point load tests and calculation methods

Obtaining the mechanical properties of rocks with poor geological conditions poses practical challenges due to the need for rapid data acquisition. The point load strength index (PLSI) test holds significant application value in various rock engineering practices such as mining engineering, tunnelling construction, support design, hydraulic engineering. In 1965, the point load test method was recommended to measure the strength of rock by the International Society for Rock Mechanics (ISRM). For irregular rocks, the ISRM suggests the following equation to calculate the PLSI (Brook 1972; Turk and Dearman 1985):

$$I_s = P \big/ D_e^2 \tag{1}$$

where I_s is the PLS (MPa), and P is the load (N) of the sample. D_e is the equivalent diameter (mm). D_e is defined as follows (Yin et al. 2017):

$$D_e = \sqrt{4WD/\pi} \ or \ D_e = \sqrt{4WD^*/\pi} \tag{2}$$

$$W = \left(W_1 + W_2\right)\big/2 \tag{3}$$

where the definitions of D, D^*, W_1 and W_2 (mm) are shown in Fig. 5.

Establishing a correction factor is imperative in PLSI tests s conducted on samples with varying sizes (Qiany and Lin 1987). The size-corrected PLSI of a rock sample is defined accordingly.

$$I_{s50} = FI_S \tag{4}$$

$$F = \left(D_e \big/ 50\right)^m \tag{5}$$

where I_s and I_{s50} are the PLS before and after correction, respectively. F is the size correction index, and m is the correction power index. The correction power index m directly affects the accuracy of point load test results.

According to the ISRM-suggested method (Franklin 1985), the size correction power index m can be obtained from either a chart or through the expression $F=(D_e/50)^{0.45}$. This implies that the correction power index m of a rock sample is 0.45. In case of samples with irregular shapes and sizes, m can be determined as follows:

$$m = 2(1 - n) \tag{6}$$

where n is the slope of the fitting line between $\lg D_e^{\ 2}$ and $\lg P$ (Forster et al. 1983).

In addition, Yin et al. (2017) proposed a new method to determine m. According to Eqs. (4) and (5), Eq. (7) can be expressed as:

$$\log\left(I_{S(50)}/I_S\right) = m \log\left(D_e/50\right) \tag{7}$$

$$m = \frac{\log\left(I_{S(50)}/I_S\right)}{\log\left(D_e/50\right)} \tag{8}$$

Using point load test data of irregular samples, the relationship between $\log(I_{s(50)}/I_s)$ and $\log(D_e/50)$ can be obtained. The slope of the linear regression line between $\log(I_{s(50)}/I_s)$ and $\log(D_e/50)$ is the power index *m.*

In this paper, the effects of two calculation methods $m_1 = 2(1 - n)$ and $m_2 = \frac{\log\left(I_{S(50)}/I_S\right)}{\log\left(D_e/50\right)}$ on the point

Fig. 6 The ore and rock samples **a** Mechanical excavation at a stope with depth of about 1000 m; **b** irregular rock samples; **c** ores and rocks with large size and good integrality; **d** standard cylindrical samples and the Brazilian disk samples

load strength index ($I_{s(50)}$) of irregular ore and rock samples are studied. The above equations can be expressed as:

$$\begin{cases} I_{s(50)-1} = F_1 I_s = \left(D_e/50\right)^{m_1} I_s \\ I_{s(50)-2} = F_2 I_s = \left(D_e/50\right)^{m_2} I_s \end{cases} \tag{9}$$

The average value of the PLSI is defined as follows:

$$\overline{I}_s = \frac{1}{n} \sum_{i=1}^{n} I_{si} \tag{10}$$

where $\overline{I}_s$ is the average PLS (MPa) and I_{si} is the PLS of the ith sample. n is the number of effective samples. When a dataset contains more than 15 values, the two highest and lowest values are excluded (Zhu et al. 2018).

3.2 Rock samples

This section outlines the procedures for preparing irregular rock samples and the accompanying test equipment. The sample preparation and test methods adhere to the standard practices suggested by ASTM (ASTM 1995, 2016; Heidari et al. 2012). The ore and rock samples were extracted from a lead–zinc mine in Yunnan Province, China. As shown in Fig. 6, irregular rock blocks (36 samples) and ore blocks (36 samples) cut using the mechanical excavation method were collected from a stope at a depth of 1000 m for the point load test. The size of the irregular samples is about 50 ± 25 mm. Irregular ore and rock samples were assigned numbers from $O1$ to $O36$ and $R1$ to $R36$, respectively. In addition to these, standard cylindrical and the Brazilian disk samples (Fig. 6d) were prepared by drilling and coring (Fig. 6c) at the same site as irregular ore and rock samples. These samples were subsequently subjected to uniaxial compression tests and the Brazilian splitting tests.

Before the uniaxial compression test, a petrological analysis was conducted on both the ore sample and surrounding rock sample to determine their mineral composition, microstructure, and grain size distribution. The results reveal that the ore sample is comprised of 60% sphalerite, 25% pyrite and 15% galena, with grain sizes of 0.1–0.5 mm, 0.03–0.2 mm, and 0.03–0.3 mm, respectively. The surrounding rock, on the other hand, consists of 96% dolomite, 4% calcite and trace amounts of clay, with grain sizes of 0.4–1.5 mm, 0.2–0.6 mm, and 0.005–0.01 mm, respectively. Their typical micrographs are shown in Fig. 7.

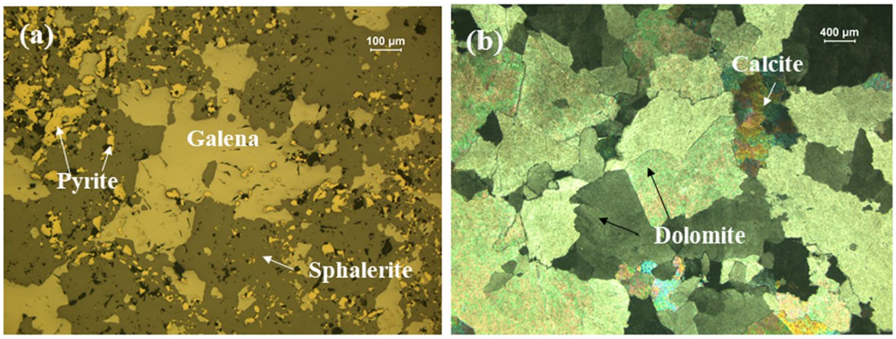

Fig. 7 Microscopic structure images: **a** ore sample, and **b** surrounding rock sample

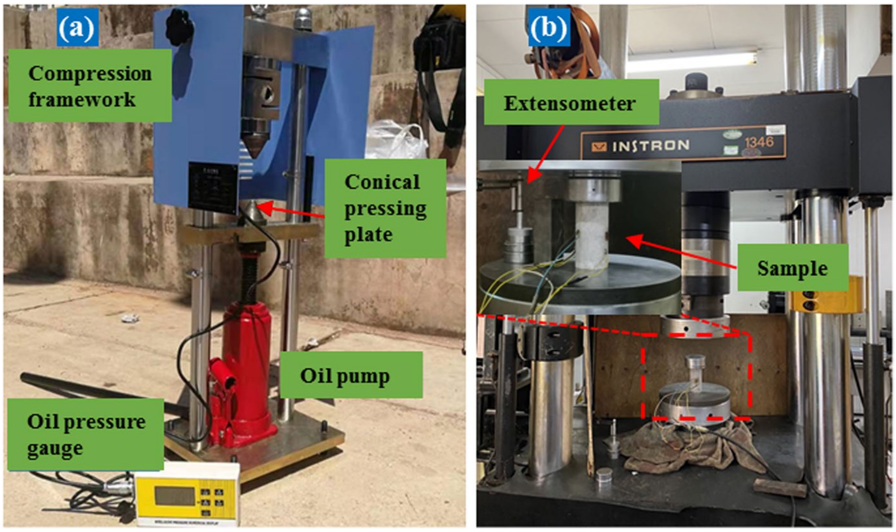

Fig. 8 Test equipment: **a** point load test instrument, **b** Instron 1346 for the uniaxial compression tests and the Brazilian splitting tests

3.3 Test equipment

As shown in Fig. 8, the LFDT-D1 digital rock point load test instrument, consisting of a loading system shake oil pump, sensing system, bearing frame and cone pressure plate, was used to conduct point load tests. The spherical conical pressure plate possesses a spherical radius of curvature of 5 mm and an apex angle of 60°. The sensing system is composed of a displacement sensor and an electronic display oil pressure gauge. Uniaxial compression tests and Brazilian splitting tests were conducted using the Instron-1346 and -1342 electrohydraulic servo compression testing systems with the maximum load of 2000 kN and 200 kN, respectively. Prior to testing, sufficient lubricant was applied to the top and bottom surfaces of the sample to reduce end friction effect. The displacement-control method at 0.4 mm/min was adopted during the test.

4 Testing results

Two correction power indexes (m_1 and m_2) are derived from distinct data-processing methods, alongside two size correction indexes (F_1 and F_2). In addition, a comparative analysis is conducted on two point load correction indexes ($I_{s(50)\text{-}1}$ and $I_{s(50)\text{-}2}$) of irregular ore rocks.

4.1 Determination of the power index m in F of irregular samples

4.1.1 Determination of $I_{s(50)\text{-}1}$ and power index m_1

The relationship between $\lg D_e^2$ and $\lg P$ of ore and rock is plotted in Fig. 9, where the slope of the fitting line is n. After obtaining n value, Eqs. (5) and (6) can be utilized to calculate the correction power index (m_1) and the size correction index (F_1) of ore

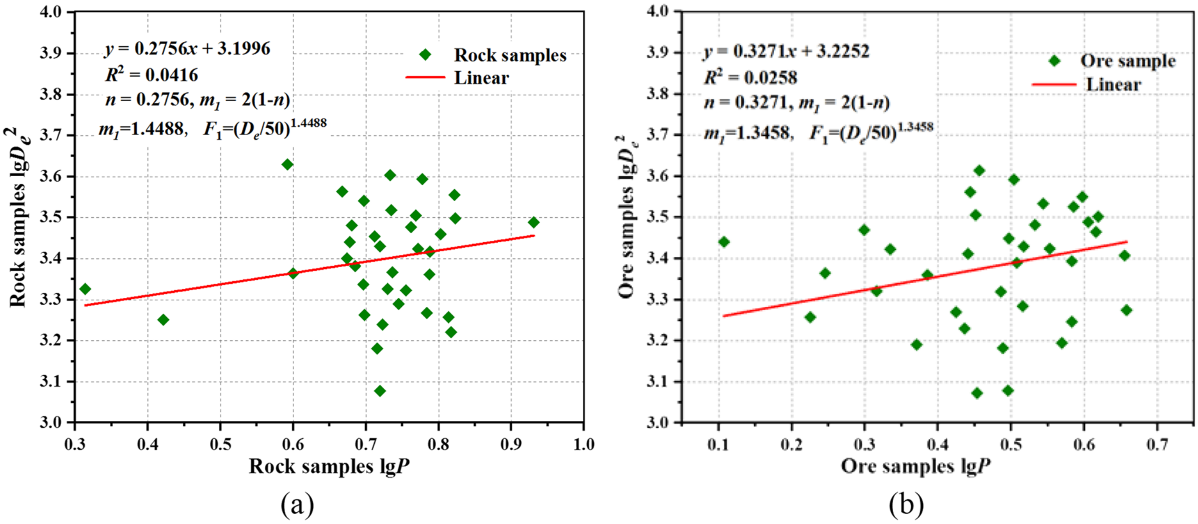

Fig. 9 Results of irregular lump point load tests on **a** irregular rock samples and **b** irregular ore samples: data and line fitting of lg(D_{e2}) against lg(P) to determine the power index m_1 of the size correction index F_1

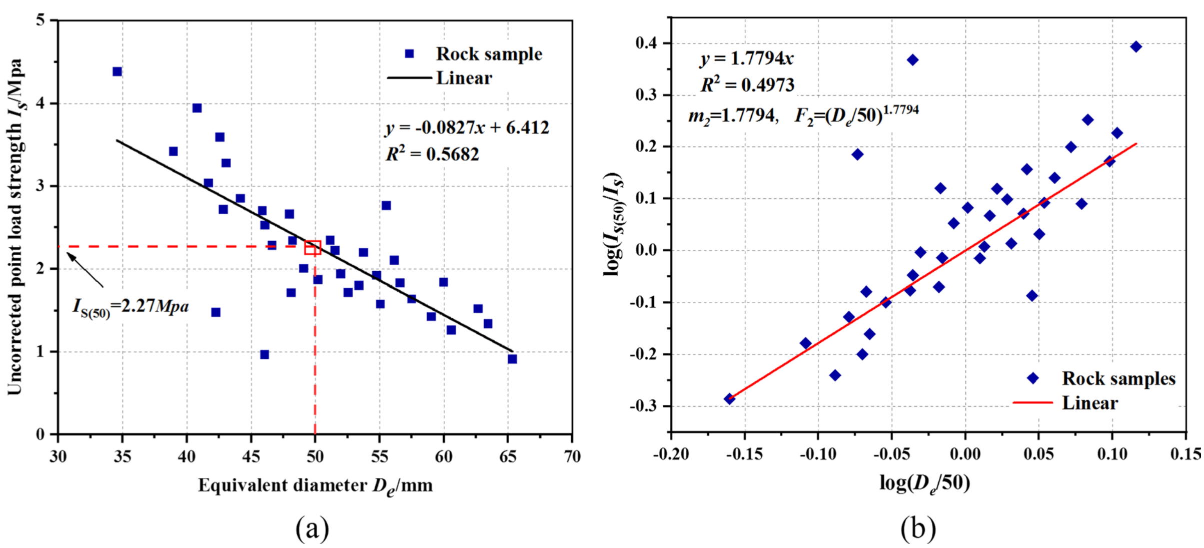

Fig. 10 Results of irregular lump point load tests on rock samples: **a** data and line fitting of uncorrected point load strength (I_s) against equivalent diameter (D_e) to determine the $I_{s(50)}$; **b** data and line fitting of log($I_{s(50)}/I_s$) against log(D_e/50) to determine the power index m_2 of the size correction index F_2

and rock samples with irregular sizes. Figure 9 illustrates that the correction power index (m_1) for ore and rock are 1.4488 and 1.3458, respectively. By applying Eq. (9), the point load strength index ($I_{s(50)\text{-}1}$) of each irregular ore and rock sample can be computed.

4.1.2 Determination of $I_{s(50)\text{-}2}$ and power index m_2

Figure 10 presents the point load test results of irregular rocks and the calculation process for m_2. The point load strength index (I_s) is calculated using Eq. (1). The uncorrected PLSI (I_s) and the equivalent diameter (D_e) of rock samples are then subjected to linear regression analysis. As shown in Fig. 10 **(a)**, a vertical line is plotted from $D_e = 50$ mm upwards to the fitting line, from which a horizontal line is plotted to determine $I_s = 2.27$ MPa. It indicates that $I_{s(50)} = 2.27$ MPa.

After obtaining $I_{s(50)}$, the relationship of $I_{s(50)}/I_s$ versus $D_e/50$ can be fitted using the power function in Eqs. (5) and (7). As plotted in Fig. 10b, to accurately determine the power index m_2, the relationship between $\log(I_{s(50)}/I_s)$ and $\log(D_e/50)$ is displayed. The slope of the fitting line is the power index m_2, which is calculated to be 1.7794. Then Eqs. (5) and (9) are adopted to obtain the size correction index F_2 and the PLSI $I_{s(50)\text{-}2}$ for each ore and rock sample. Figure 11 shows the point load test results of irregular ore samples and the calculation process of m_2. The power index m and the size correction index F of ore and rock obtained by the two data analysis methods are listed in Table 1.

4.2 Point load test results of irregular samples

The point load test results of each irregular ore samples and rock samples are provided in Tables 2 and 3, respectively. The point load strength (I_s) of ore samples and rock samples varies significantly, ranging from 0.46 to 2.61 MPa and from 0.92 to 4.39 MPa, respectively. The average value of $I_{s(50)}$ are obtained using two correction methods and listed in Table 4.

Table 1 Calculation results of the power index m and the size correction index F

Samples	m_1	F_1	m_2	F_2
Rock samples	1.4488	$(D_e/50)^{1.4488}$	1.7794	$(D_e/50)^{1.7794}$
Ore samples	1.3458	$(D_e/50)^{1.3458}$	1.6978	$(D_e/50)^{1.6978}$

As shown in Table 4, the point load strengths obtained by the two data analysis methods are close to each other. The average value of $I_{s(50)\text{-}1}$ and $I_{s(50)\text{-}2}$ of rock samples are 2.15 MPa and 2.14 MPa, respectively, and the counterparts for ore samples are 1.26 MPa and 1.25 MPa, respectively. The point load indexes $I_{s(50)\text{-}1}$ and $I_{s(50)\text{-}2}$ obtained by the two correction methods are consistent with those obtained using the method recommended by the ISRM (1985). This can be attributed to the selection of samples with comparable dimensions (equivalent diameter close to 50 mm).

5 Discussion

5.1 Correlation between PLSI and equivalent diameter

Figure 12 depicts the relationship between the uncorrected point load strength (I_s) and the equivalent

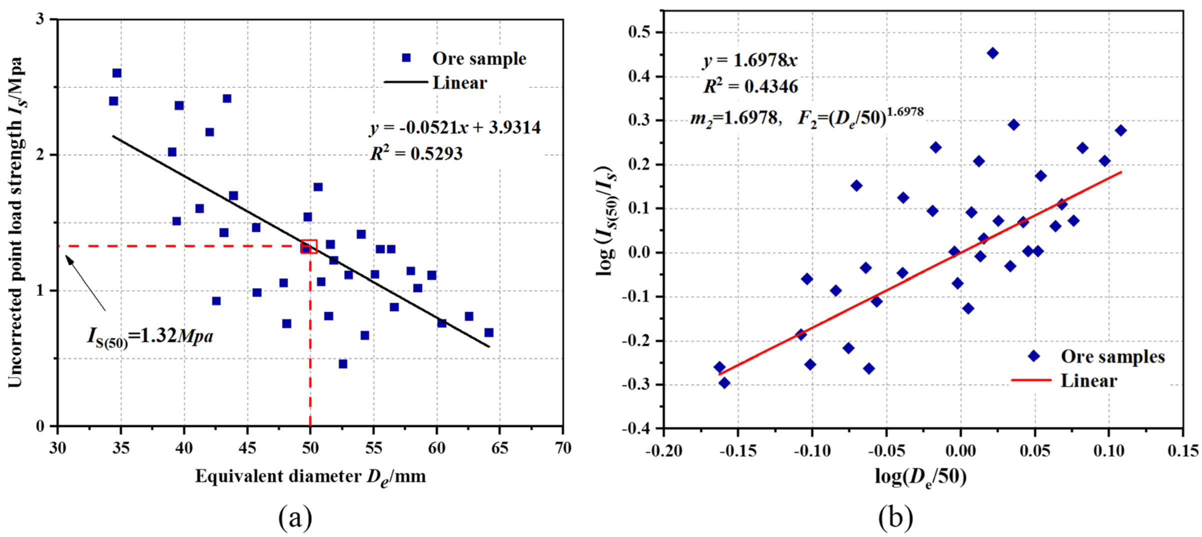

Fig. 11 Results of irregular lump point load tests on ore samples: **a** data and line fitting of uncorrected point load strength (I_s) against equivalent diameter (D_e) to determine the $I_{s(50)}$; **b** data and line fitting of $\log(I_{s(50)}/I_s)$ against $\log(D_e/50)$ to determine the power index m_2 of the size correction index F_2

Table 2 Point load test results of irregular ore samples

Samples on	D (mm)	W (mm)	P (KN)	De (mm)	Is (MPa)	$I_{s(50)}=Is\,(De/50)^{0.45}$	F_1	$I_{s(50)\text{-}1}$ (MPa)	F_2	$I_{s(50)\text{-}2}$ (MPa)	Discarded value
$O1$	48.85	66.03	2.86	64.10	0.70	0.78	1.40	0.97	1.52	1.06	
$O2$	43.95	69.82	3.19	62.52	0.82	0.90	1.35	1.10	1.46	1.19	
$O3$	46.94	44.42	3.57	51.54	1.34	1.36	1.04	1.40	1.05	1.41	
$O4$	30.08	48.56	2.66	43.14	1.43	1.34	0.82	1.17	0.78	1.11	
$O5$	48.07	41.78	4.52	50.58	1.77	1.78	1.02	1.79	1.02	1.80	
$O6$	43.64	57.14	4.16	56.36	1.31	1.38	1.17	1.54	1.23	1.60	
$O7$	36.98	52.54	3.83	49.75	1.55	1.54	0.99	1.54	0.99	1.53	
$O8$	44.01	65.03	2.78	60.38	0.76	0.83	1.29	0.98	1.38	1.05	
$O9$	28.49	43.17	3.71	39.58	2.37	2.13	0.73	1.73	0.67	1.59	
$O10$	30.75	46.18	1.68	42.53	0.93	0.86	0.80	0.75	0.76	0.71	
$O11$	39.37	52.73	2.16	51.43	0.82	0.83	1.04	0.85	1.05	0.86	
$O12$	41.21	57.80	3.41	55.08	1.12	1.17	1.14	1.28	1.18	1.32	
$O13$	45.26	53.43	4.03	55.50	1.31	1.37	1.15	1.51	1.19	1.56	
$O14$	39.01	46.56	1.76	48.10	0.76	0.75	0.95	0.72	0.94	0.71	
$O15$	27.51	53.65	4.55	43.36	2.42	2.27	0.83	2.00	0.79	1.90	▲
$O16$	36.43	76.46	3.96	59.57	1.12	1.21	1.27	1.41	1.35	1.50	
$O17$	33.48	60.57	2.76	50.83	1.07	1.08	1.02	1.09	1.03	1.10	
$O18$	29.67	50.96	3.28	43.89	1.70	1.61	0.84	1.43	0.80	1.36	
$O19$	46.40	57.81	3.5	58.46	1.02	1.10	1.23	1.26	1.30	1.34	
$O20$	37.86	69.55	3.85	57.92	1.15	1.23	1.22	1.40	1.28	1.47	
$O21$	36.10	33.09	3.08	39.01	2.02	1.81	0.72	1.45	0.66	1.33	
$O22$	40.06	48.04	3.22	49.51	1.31	1.31	0.99	1.30	0.98	1.29	
$O23$	34.46	47.5	3.06	45.66	1.47	1.41	0.89	1.30	0.86	1.26	
$O24$	27.65	33.57	2.84	34.39	2.40	2.03	0.60	1.45	0.53	1.27	
$O25$	31.84	66.22	3.29	51.83	1.22	1.24	1.05	1.29	1.06	1.30	
$O26$	45.61	48.33	3.14	52.99	1.12	1.15	1.08	1.21	1.10	1.23	
$O27$	31.05	52.87	2.07	45.73	0.99	0.95	0.89	0.88	0.86	0.85	
$O28$	33.00	41.95	3.83	41.99	2.17	2.01	0.79	1.72	0.74	1.61	
$O29$	50.72	45.60	1.99	54.28	0.68	0.70	1.12	0.75	1.15	0.78	▲
$O30$	43.51	57.82	2.83	56.61	0.88	0.93	1.18	1.04	1.23	1.09	
$O31$	22.57	53.94	2.35	39.38	1.52	1.36	0.73	1.10	0.67	1.01	
$O32$	30.80	43.24	2.73	41.19	1.61	1.47	0.77	1.24	0.72	1.16	
$O33$	44.83	51.03	4.13	53.98	1.42	1.47	1.11	1.57	1.14	1.61	
$O34$	47.13	45.97	1.28	52.54	0.46	0.47	1.07	0.50	1.09	0.50	▲
$O35$	33.26	54.04	2.43	47.85	1.06	1.04	0.94	1.00	0.93	0.98	
$O36$	27.40	34.40	3.13	34.65	2.61	2.21	0.61	1.59	0.54	1.40	▲

▲ indicates the failure data

diameter (D_e) of irregular ore and rock samples. It is evident that there is a notable negative correlation between them, i.e., the point load strength decreases with increasing equivalent diameter. This variation trend is consistent with the findings of Masoumi et al. (2018) who carried out point load tests on regular rock samples.

Table 3 Point load test results of irregular rock samples

Samples on	D (mm)	W (mm)	P (KN)	De (mm)	Is (MPa)	$I_{s(50)}=Is\,(De/50)^{0.45}$	F_1	$I_{s(50)\text{-}1}$ (MPa)	F_2	$I_{s(50)\text{-}2}$ (MPa)	Discarded value
$R1$	35.47	46.93	5.37	46.05	2.53	2.44	0.89	2.25	0.86	2.19	
$R2$	39.16	63.16	6.65	56.13	2.11	2.22	1.18	2.50	1.23	2.59	
$R3$	27.33	34.32	5.24	34.57	4.39	3.71	0.59	2.57	0.52	2.27	▲
$R4$	37.14	38.73	4.99	42.81	2.72	2.54	0.80	2.17	0.76	2.07	
$R5$	54.72	57.66	5.41	63.40	1.35	1.50	1.41	1.90	1.53	2.05	
$R6$	36.43	35.82	6.56	40.77	3.95	3.60	0.74	2.94	0.70	2.74	▲
$R7$	38.21	47.75	5.45	48.21	2.34	2.31	0.95	2.22	0.94	2.20	
$R8$	26.55	54.75	6.08	43.03	3.28	3.07	0.80	2.64	0.77	2.51	
$R9$	37.92	68.38	5.43	57.47	1.64	1.75	1.22	2.01	1.28	2.11	
$R10$	48.28	58.44	6.63	59.95	1.84	2.00	1.30	2.40	1.38	2.55	
$R11$	35.39	53.42	4.84	49.07	2.01	1.99	0.97	1.96	0.97	1.94	
$R12$	40.21	51.02	6.14	51.12	2.35	2.37	1.03	2.43	1.04	2.44	
$R13$	28.09	58.76	5.69	45.85	2.71	2.60	0.88	2.39	0.86	2.32	
$R14$	45.61	37.37	4.97	46.60	2.29	2.22	0.90	2.07	0.88	2.02	
$R15$	29.78	55.84	2.06	46.03	0.97	0.94	0.89	0.86	0.86	0.84	▲
$R16$	36.19	32.89	5.19	38.94	3.42	3.06	0.70	2.38	0.64	2.19	
$R17$	29.98	46.70	2.64	42.23	1.48	1.37	0.78	1.16	0.74	1.10	
$R18$	33.94	53.47	3.98	48.08	1.72	1.69	0.94	1.63	0.93	1.61	
$R19$	27.38	51.90	6.51	42.55	3.60	3.34	0.79	2.85	0.75	2.70	
$R20$	54.16	61.82	3.91	65.31	0.92	1.03	1.47	1.35	1.61	1.47	▲
$R21$	39.78	34.25	5.28	41.66	3.04	2.80	0.77	2.34	0.72	2.20	
$R22$	41.91	49.68	5.91	51.50	2.23	2.26	1.04	2.33	1.05	2.35	
$R23$	42.9	52.81	6.35	53.72	2.20	2.27	1.11	2.44	1.14	2.50	
$R24$	45.92	51.76	4.79	55.03	1.58	1.65	1.15	1.82	1.19	1.88	
$R25$	45.44	53.19	8.53	55.49	2.77	2.90	1.16	3.22	1.20	3.33	
$R26$	43.88	41.16	6.13	47.97	2.66	2.62	0.94	2.51	0.93	2.47	
$R27$	40.46	48.83	4.72	50.17	1.88	1.88	1.00	1.88	1.01	1.89	
$R28$	37.33	58.03	4.76	52.53	1.72	1.76	1.07	1.85	1.09	1.88	
$R29$	51.3	60.04	5.99	62.64	1.53	1.69	1.39	2.12	1.49	2.28	
$R30$	52.06	48.23	5.87	56.56	1.84	1.94	1.20	2.19	1.25	2.29	
$R31$	43.68	51.2	5.15	53.38	1.81	1.86	1.10	1.99	1.12	2.03	
$R32$	49.89	54.75	4.98	58.99	1.43	1.54	1.27	1.82	1.34	1.92	
$R33$	40.09	52.81	5.24	51.93	1.94	1.98	1.06	2.05	1.07	2.08	
$R34$	45.52	63.2	4.65	60.54	1.27	1.38	1.32	1.67	1.41	1.78	
$R35$	29.39	52.03	5.56	44.14	2.85	2.70	0.83	2.38	0.80	2.29	
$R36$	50.89	46.25	5.78	54.76	1.93	2.01	1.14	2.20	1.18	2.27	

▲ indicates the failure data

Figure 13 shows the relationship between $I_{s(50)\text{-}1}$ and $I_{s(50)\text{-}2}$ for irregular ore and rock samples using two different correction methods. $I_{s(50)\text{-}1}$ and $I_{s(50)\text{-}2}$ exhibit significant discreteness. The results of rock samples are mainly between 1.75 and 2.75 MPa, while those of ore samples are primarily within the range of 1.00 to 1.60 MPa. The discrepancy $\Delta I_{s(50)}$ is defined as follows:

$$\Delta I_{s(50)} = I_{S(50)-1} - I_{S(50)-2} \tag{11}$$

Table 4 I_s average values for the ore and rock blocks (average value)

Samples	Is (MPa)	$I_{s(50)}=Is$ (De/50) $^{0.45}$ (ISRM)	$I_{s(50)\text{-}1}$ (MPa)	$I_{s(50)\text{-}2}$ (MPa)
Rock samples	2.23	2.09	2.15	2.14
Ore samples	1.34	1.31	1.26	1.25

As depicted in Fig. 13, when the equivalent diameter $D_e=50$ mm, $I_{s(50)\text{-}1}$ is equivalent to $I_{s(50)\text{-}2}$, signifying that $\Delta I_{s(50)}=0$. This implies that the equivalent diameter (D_e) of ore and rock samples significantly affects the corrected PLSI. When the equivalent diameter is approximately 50 mm, the correction result of the PLSI will be more accurate. If the size of ore and rock samples is either larger or smaller, the error of the results using different correction methods will be larger.

In practical engineering applications, it is recommended to select irregular rock samples with an equivalent diameter of approximately 50 mm for point load strength tests to accurately predict UCS. In addition, it should be noted that the $\lg D_e^2$ and lgP data do not conform to a linear relationship (Fig. 9). As a consequence, the value of the slope of the line (parameter n) is quite controversial, and the assumed correction power index (m_1), size correction index (F_1) and point load strength index ($I_{s(50)\text{-}1}$) values have certain limitations. However, $I_{s(50)\text{-}2}$ can be used to calculate the PLSI of irregular samples is considered more stable than $I_{s(50)\text{-}1}$ within a certain equivalent diameter range.

5.2 Effect of excavation method on PLSI of rocks

The stress state of surrounding rocks will undergo a redistribution process after the excavation of a roadway in deep hard rocks. Different excavation techniques employed will result in varying degrees of damage to surrounding rock masses (He 2006; Ranjith et al. 2017). Opting for an appropriate excavation method is of great significance for ensuring safe and efficient deep mining. It is imperative to select suitable excavation and mining methods that minimize the damage to rock masses and guarantee the stability of both the stope and surrounding rocks (Wang et al. 2022; Fan et al. 2016).

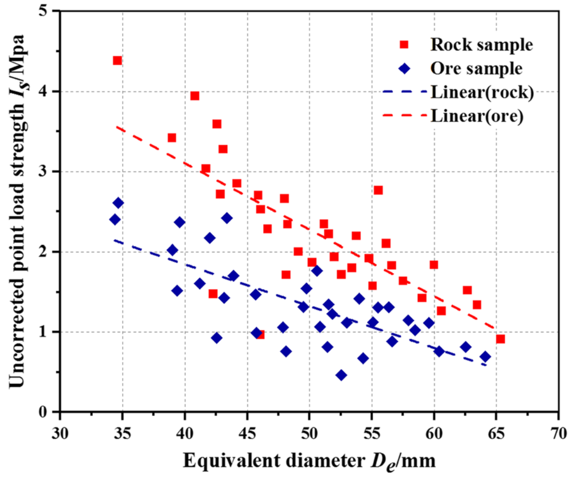

Fig. 12 The relationship between uncorrected point load strength (I_s) and equivalent diameter (D_e) of irregular ore and rock samples

In our previous study (Li et al. 2021), the PLSI values were acquired for irregular ore and rock blocks that were produced through the drilling and blasting method. It should be noted that both the drilling and blasting method and the mechanical excavation method were employed at identical depths and formations for the present mining project. The point load strength indexes $I_{s(50)}$ of irregular ore and rock samples generated by different tunneling methods are listed in Table 5.

The point load strengths of ore and rock samples generated by the drilling-blasting method are 0.39 MPa and 1.33 MPa, respectively, only 31.20% and 62.15% of the values using the mechanical method, respectively. This indicates that, under the same geological conditions, the mechanical excavation method causes less damage to surrounding rocks than the drilling-blasting excavation method. When using the to predict the UCS of rocks in deep mining engineering, the influence of excavation method on the damage to rock masses should be taken into account. Hence, in point load tests, it is advisable to select ore and rock blocks that exhibit minimal blasting disturbance and lower damage degree, as this will help to mitigate the impact of external disturbance on the test results. In practice, the mechanical excavation method can effectively reduce the damage from engineering disturbance to rocks and enhance the stability of surrounding rock masses (Fan et al. 2016; Ranjith et al. 2017).

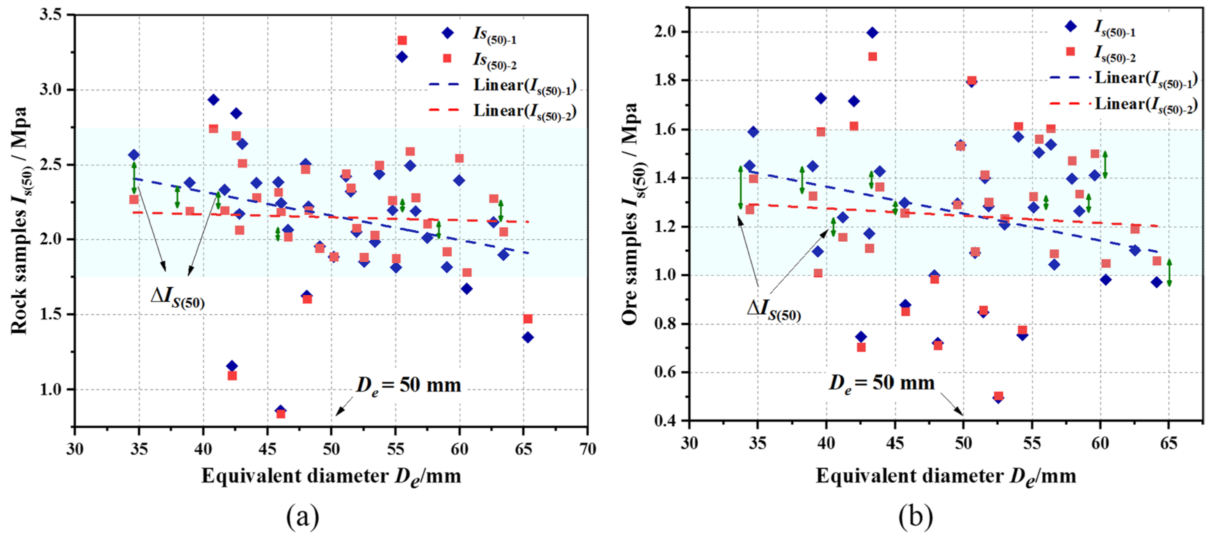

Fig. 13 The relationship between $I_{s(50)\text{-}1}$ and $I_{s(50)\text{-}2}$ and the equivalent diameter (D_e) for **a** irregular rock samples; and **b** irregular ore samples

Table 5 Point load strength index of ore and rock samples under two excavation methods

Samples	Excavation method	Number of tests	Average $I_{s(50)}$(MPa)
Rock samples	Drilling-blasting method	30	1.33
	Mechanical method	36	2.14
Ore samples	Drilling-blasting method	30	0.39
	Mechanical method	36	1.25

5.3 Correlation between UCS (BTS) and PLSI

As described in Sect. 3.2, both standard cylindrical and Brazilian disk samples were prepared by drilling and coring at the same location with irregular ore and rock samples. However, owing to the presence of weak planes and defects, only a few standard samples were produced for UCS and tensile tests (4 cylindrical samples and 4 Brazilian disc samples). Figure 14

Fig. 14 Typical failure photos of rock and ore samples after uniaxial compression and Brazilian splitting tests

Table 6 Conversion factors (k) of the rocks and ores for UCS and BTS (average value)

Samples	Density (Kg/m^3)	Elastic modulus(GPa)	UCS(MP)	BTS(MPa)	$I_{s(50)}$ (MPa)	k for UCS	k for BTS
Rock	2778.05	30.97	100.11	5.98	2.14	46.78	2.79
Ore	4540.87	21.81	73.58	3.88	1.25	58.86	3.10

shows the typical failure patterns of ore and rock samples after uniaxial compression and Brazilian tensile tests. The UCS and BTS (average values) of the samples are listed in Table 6.

A commonly accepted regression equation for the UCS determination by $I_{s(50)}$ is as follows (Azimian et al. 2014; Singh et al. 2012):

$$UCS = kI_{S(50)} \tag{12}$$

where k is the strength conversion factor. A prediction equation similar to Eq. (11) can be used to correlate the relationship between BTS and $I_{s(50)}$ (Li et al. 2013). Based on Eqs. (4) and (5), the correlation between I_s and UCS can be expressed as follows:

$$UCS = kI_s\left(D_e/50\right)^m \tag{13}$$

In recent years, there has been extensive experimental research conducted on the k value of various rock types (Kahraman 2014; Koohmishi and Sciences 2021). The average UCS values of the ore and rock are 100.11 MPa and 73.58 MPa, respectively. The k value can be determined using the regression Eq. (11) based on the results from uniaxial compression and the Brazilian splitting tests. The corresponding conversion factors (k) and $I_{s(50)}$ of the ore and rock are listed in Table 6. It should be noted that $I_{s(50)}$ in Table 6 corresponds to $I_{s(50)\text{-}2}$ in the paper.

The correlation factors for irregular ore and rock lumps between BTS and $I_{s(50)}$ are 2.79 and 3.10, respectively. The conversion factors (k) for the USC of ore and rock are 46.78 and 58.86, respectively, which highly exceed the ISRM-suggested value of 20–25 (1985). In deep mining, dynamic disturbances such as mechanical excavation and blasting vibration cause internal damage to ore and rock samples, leading to a reduction in the point load strength of irregular ore and rock samples. In this case, the correlation factors (k) between PLSI ($I_{s(50)}$) and USC, recommended by ISRM and ASTM used to predict the UCS of ore and rock, tends to remarkably underestimate the actual UCS of ore and rock.

6 Conclusions

The PL tests were carried out on irregular ore and rock samples in a stope at a depth of about 1000 m in a lead–zinc mine with poor geological conditions. The following conclusions are obtained:

(1) The uncorrected point load strength index (I_s) of irregular ore and rock samples exhibits a conspicuous size effect, whereby I_s decreases with the increase of equivalent diameter (D_e).
(2) The point load strength indexes ($I_{s(50)\text{-}1}$ and $I_{s(50)\text{-}2}$) of irregular ore and rocks from two different correction methods vary. The two corrected PLSIs of $I_{s(50)\text{-}1}$ and $I_{s(50)\text{-}2}$ are essentially equal when the equivalent diameter is approximately 50 mm.
(3) The excavation method significantly affects the $I_{s(50)}$ of ore and rock samples. The $I_{s(50)}$s of ore and rock samples generated by the drilling-blasting method are only 31.20% and 62.15% of those of corresponding samples generated by the mechanical method, respectively. This indicates that the $I_{s(50)}$ obtained by the mechanical excavation method is close to the actual value of ore and surrounding rock.
(4) The correlation factors between the UCS and the $I_{s(50)}$ of irregular ore and rock lumps are 45.71 and 58.86, respectively. The correlation factors (k) recommended by ISRM and ASTM tend to remarkably underestimate their actual UCSs after mining excavation disturbance.

Author contribution PL, DL and XF: Conceptualization, Methodology. PL: Data curation, Writing-Original draft preparation. PL: Visualization, Investigation. DL, YY and HL:

Project administration. PC and JM: Resources. DL: Writing—Reviewing and Editing, Funding acquisition.

Funding The authors would like to acknowledge the financial support from the National Natural Science Foundation of China (No. 52074349). The authors would like to express appreciation to Dr. Zhenyu Han at Monash University for editing the English language in the revision process.

Data availability The data that support the findings of this study are available from the corresponding author, [Diyuan Li], upon reasonable request.

Declarations

Competing interests The authors declare that they have no known competing financial interests or personal relationships that could have appeared to influence the work reported in this paper.

Ethical approval Not applicable, Ethics approval was not required for this research.

Consent to publish All authors consent to the publication of this paper.

References

Aladejare AE, Akeju VO, Wang Y (2022) Data-driven characterization of the correlation between uniaxial compressive strength and Youngs' modulus of rock without regression models. Transp Geotech 32:100680

ASTM (1995) Standard test method for determination of the point load strength index of rock. Am Soc Test Mater 22:1–9

ASTM (2016) Standard test method for determination of the point load strength index of rock and application to rock strength classifications. ASTM Int West Conshohocken. D5731–16

Azimian A, Ajalloeian R, Fatehi L (2014) An empirical correlation of uniaxial compressive strength with P-wave velocity and point load strength index on marly rocks using statistical method. Geotech Geol Eng 32:205–214

Basu A (2008) The point load test in rock material characterization. Eng Geol 35:379–387

Basu A, Aydin A (2006) Predicting uniaxial compressive strength by point load test: significance of cone penetration. Rock Mech Rock Eng 39(5):483–490

Basu A, Kamran M (2010) Point load test on schistose rocks and its applicability in predicting uniaxial compressive strength. Int J Rock Mech Min Sci 47(5):823–828

Bieniawski Z (1975) The point-load test in geotechnical practice. Eng Geol 9(1):1–11

Broch E, Franklin J (1972) The point-load strength test. Int J Rock Mech Min Sci Geomech Abstr. 9(6):669–676

Brook N (1972) The equivalent core diameter method of size and shape correction in point load testing. Int J Rock Mech Min Sci Geomech Abstr. 22(2):61–70

Brook N (1980) Size correction for point load testing. Int J Rock Mech Min Sci Geomech Abstr. 17(4):231

Çobanoğlu İ, Çelik S (2008) Estimation of uniaxial compressive strength from point load strength, schmidt hardness and P-wave velocity. Bull Eng Geol Env 67(4):491–498

Diamantis K, Gartzos E, Migiros G (2009) Study on uniaxial compressive strength, point load strength index, dynamic and physical properties of serpentinites from Central Greece: test results and empirical relations. Eng Geol 108(3–4):199–207

Fan Y, Lu W, Zhou Y, Yan P, Leng Z, Chen M (2016) Influence of tunneling methods on the strainburst characteristics during the excavation of deep rock masses. Eng Geol 201:85–95

Fener M, Kahraman S, Bilgil A, Gunaydin O (2005) A comparative evaluation of indirect methods to estimate the compressive strength of rocks. Rock Mech Rock Eng 38(4):329–343

Feng X-T, Gao Y, Zhang X, Wang Z, Zhang Y, Han Q (2020) Evolution of the mechanical and strength parameters of hard rocks in the true triaxial cyclic loading and unloading tests. Int J Rock Mech Min Sci 131:104349

Forster I (1983) The influence of core sample geometry on the axial point-load test. Int J Rock Mech Min Sci Geomech Abstr. 20(6)

Franklin J (1985) Suggested method for determining point load strength. Int J Rock Mech Min Sci Geomech Abstr 22(2):51–60

Han R, Wang F, Hu Y, Wang X, Ren T, Qiu W, Zhong K (2014) Metallogenic tectonic dynamics and chronology constrains on the Huize-type (HZT) germanium-rich silver-zinc-lead deposits. Geotecton Metallog 38(4):758–771

Han Z, Li D, Li X (2022) Effects of axial pre-force and loading rate on mode I fracture behavior of granite. Int J Rock Mech Min Sci 157:105172

Han Z, Li J, Wang H, Zhao J (2023) Initiation and propagation of a single internal 3D crack in brittle material under dynamic loads. Eng Fract Mech 285:109299

He MC (2006) Rock mechanics and hazard control in deep mining engineering in China. 29–46

Heidari M, Khanlari G, Torabi Kaveh M, Kargarian S (2012) Predicting the uniaxial compressive and tensile strengths

of gypsum rock by point load testing. Rock Mech Rock Eng 45(2):265–273
ISRM (1985) Suggested method for determining point load strength. Int J Rock Mech Min Sci Geomech Abstr 22(2):51–60
Kahraman S (2014) The determination of uniaxial compressive strength from point load strength for pyroclastic rocks. Eng Geol 170:33–42
Kahraman S, Gunaydin O (2009) The effect of rock classes on the relation between uniaxial compressive strength and point load index. Bull Eng Geol Env 68(3):345–353
Khanlari G-R, Heidari M, Sepahigero A-A, Fereidooni D (2014) Quantification of strength anisotropy of metamorphic rocks of the Hamedan province, Iran, as determined from cylindrical punch, point load and Brazilian tests. Eng Geol 169:80–90
Kohno M, Maeda H (2012) Relationship between point load strength index and uniaxial compressive strength of hydrothermally altered soft rocks. Int J Rock Mech Min Sci 50:147–157
Koohmishi M (2021) Assessment of strength of individual ballast aggregate by conducting point load test and establishment of classification method. Int J Rock Mech Min Sci 141:104711
Li D, Cai R, Yu Y, Wang Y, Li Hua (2021) Distribution characteristics of point load strength index of irregular ore rock samples in deep mine. Chinese J Eng. 2095–9389
Li D, Wong LNY (2013) Point load test on meta-sedimentary rocks and correlation to UCS and BTS. Rock Mech Rock Eng 46(4):889–896
Li Y-M, Zhao G-F (2021) A numerical integrated approach for the estimation of the uniaxial compression strength of rock from point load tests. Int J Rock Mech Min Sci 148:104939
Liu G, Xiao FK, Guo ZB (2018) Plastic characteristics of rock under point load. Sci Technol Eng 02:217–222
Masoumi H, Roshan H, Hedayat A, Hagan PC (2018) Scale-size dependency of intact rock under point-load and indirect tensile Brazilian testing. Int J Geomech 18(3):04018006
Mohamad J, Hasbollah DA, Taib AM, Dan M, Jusoh S, Said KM (2022) Correlation between uniaxial compressive strength and point load strength of penang island granites. IOP Conf Series Earth Environ Sci 971(1):012025
Protodyakonov M (1960) New methods of determining mechanical properties of rock. In: Proceedings of the International Conference on Strata Control. t87–195
Qiany BL, Lin Y (1987) Stress analysis of rock plate in irregular shape under double-point loading. J Northeastern Univ 8:312
Rabat Á, Cano M, Tomás R, Tamayo ÁE, Alejano LR (2020a) Evaluation of strength and deformability of soft sedimentary rocks in dry and saturated conditions through needle penetration and point load tests: a comparative study. Rock Mech Rock Eng 53(6):2707–2726
Rabat Á, Tomás R, Cano M (2020b) Evaluation of mechanical weakening of calcarenite building stones due to environmental relative humidity using the vapour equilibrium technique. Eng Geol 278:105849
Ranjith PG, Zhao J, Ju M, De Silva RV, Rathnaweera TD, Bandara AK (2017) Opportunities and challenges in deep mining: a brief review. Engineering 3(4):546–551
Robertson BB, Almond PC, Carrick ST, Penny V, Eger A, Chau HW, Smith CM (2021) The influence of rock fragments on field capacity water content in stony soils from hard sandstone alluvium. Geoderma 389:114912
Şahin M, Ulusay R, Karakul H (2020) Point load strength index of half-cut core specimens and correlation with uniaxial compressive strength. Rock Mech Rock Eng 53:3745–3760
Sarici DE, Ozdemir E (2018) Determining point load strength loss from porosity, schmidt hardness, and weight of some sedimentary rocks under freeze–thaw conditions. Environ Earth Sci 77(3):1–9
Singh T, Kainthola A, Venkatesh A (2012) Correlation between point load index and uniaxial compressive strength for different rock types. Rock Mech Rock Eng 45(2):259–264
Su Z, Tan X, Chen W, Jia H, Xu F (2021) A model of unfrozen water content in rock during freezing and thawing with experimental validation by nuclear magnetic resonance. J Rock Mech Geotech Eng. 14:1545–1555
Turk N, Dearman W (1985) Improvements in the determination of point load strength. Bull Int Assoc Eng Geol Bull De L'association Internationale De Géologie De L'ingénieur 31(1):137–142
Wang X, Li J, Zhao X, Liang Y (2022) Propagation characteristics and prediction of blast-induced vibration on closely spaced rock tunnels. Tunn Undergr Space Technol 123:104416
Wong RH, Chau KT, Yin J-H, Lai DT, Zhao G-S (2017) Uniaxial compressive strength and point load index of volcanic irregular lumps. Int J Rock Mech Min Sci 93:307–315
Xiao P, Li D, Zhao G, Liu H (2021) New criterion for the spalling failure of deep rock engineering based on energy release. Int J Rock Mech Min Sci 148:104943
Xie W-Q, Zhang X-P, Liu Q-S, Tang S-H, Li W-W (2021) Experimental investigation of rock strength using indentation test and point load test. Int J Rock Mech Min Sci 139:104647
Yin J-H, Wong RH, Chau KT, Lai DT, Zhao G-S (2017) Point load strength index of granitic irregular lumps: Size correction and correlation with uniaxial compressive strength. Tunn Undergr Space Technol 70:388–399
Zhang Q, Dai F, Liu Y (2022) Experimental assessment on the dynamic mechanical response of rocks under cyclic coupled compression-shear loading. Int J Mech Sci 216:106970
Zhou K, Dou L, Li X, Song S, Cao J, Jinzheng B, Ma X (2022) Coal burst and mining-induced stress evolution in a deep isolated main entry area–A case study. Eng Fail Anal 137:106289
Zhu J, Luo Q, Zhan X (2018) An equivalent area method for evaluating the point load strength of irregular soft phyllite. Chin J Rock Mech Eng 37(12):2762–2771
Zou J, Wu K, Zhang X (2022) Effective evaluation of deep-hole blasting for controlling strong tremors induced by deep coal mining-A case study. Int J Rock Mech Min Sci 159:105211